Electronic Supplementary Material (ESI) for Environmental Science: Nano.
This journal is © The Royal Society of Chemistry 2019

Iron oxide and zinc oxide engineered nanoparticles toxicity on *Bacillus subtilis* in freshwater systems

Supporting Information

Samuel K. Learenga[a], Eunice Ubomba-Jaswa[b], Ndeke Musee[a*1]

[a]Emerging Contaminants Ecological and Risk Assessment (ECERA) Group, Department of Chemical Engineering, University of Pretoria, Private Bag X20, Hatfield 0028, Pretoria, South Africa

[b]Water Research Commission (WRC), Pretoria, South Africa

**Corresponding author: Ndeke Musee; Email: Ndeke.musee@up.ac.za; museen2012@gmail.com[1]

Freshwater analysis

The chemical analysis of freshwater samples (Table 1) was performed in a certified laboratory (based on the South African National Accreditation System, SANAS) using the following standard analytical methods. The anions of Cl^-, NO_3^-, SO_4^{2-}, PO_4^{3-} and cations of Na^+, K^+, NH_4^+, Ca^{2+}, Mg^{2+} in the water samples were determined using the colorimetric methods and inductively coupled plasma- optical emission spectroscopy analysis, respectively. pH and electrical conductivity were measured by potentiometric determination (pH meter) whilst the DOC was determined by high temperature combustion using a Shimadzu – Total Organic Carbon analyzer.

Table S1

Hydrodynamic diameter and zeta potential of ENMs in river water samples

	nZnO (20 mg/L)		**nFe_2O_3 (5 mg/L)**	
Parameter	**Bloubank river**	**Elands river**	**Bloubank river**	**Elands river**
ζ^a (mV)	-13.41 ± 0.44	-15.07 ± 0.63	-12.25 ± 1.25	-15.12 ± 1.25
D_h^b (nm), 0 hrs	1 069 ± 187	512 ± 22	1 056 ± 120	958 ± 188
D_h (nm), 2 hrs	1 372 ± 257	558 ± 28	1 627 ± 194	1 099 ± 287

Data is presented as average ± standard deviation (n=3). [a] Zeta potential; [b] Hydrodynamic diameter.

Table S2: Zn distribution calculated by VMINTEQ from dissolved Zn concentrations measured by ICP-MS in BR and ER water.

	0.183 mgL^{-1}	**0.366 mgL^{-1}**
Species	BR water (% of total concentration)	ER water (% of total concentration)
Zn^{2+}	43.356	46.504
/FA-Zn+2G(aq)	0.170	0.382
ZnOH+	2.748	5.008
$Zn(OH)_2$ (aq)	2.558	7.564
$ZnCl^+$	0.033	0.052
$ZnSO_4$ (aq)	0.291	0.562
$ZnNH_3^{2+}$	0.054	0.115
$ZnHPO_4$ (aq)	1.029	0.810
/FAZn+(aq)	11.087	14.130
/FA2Zn(aq)	38.673	24.869
Tot DOC Zn complex	49.76%	38.999%

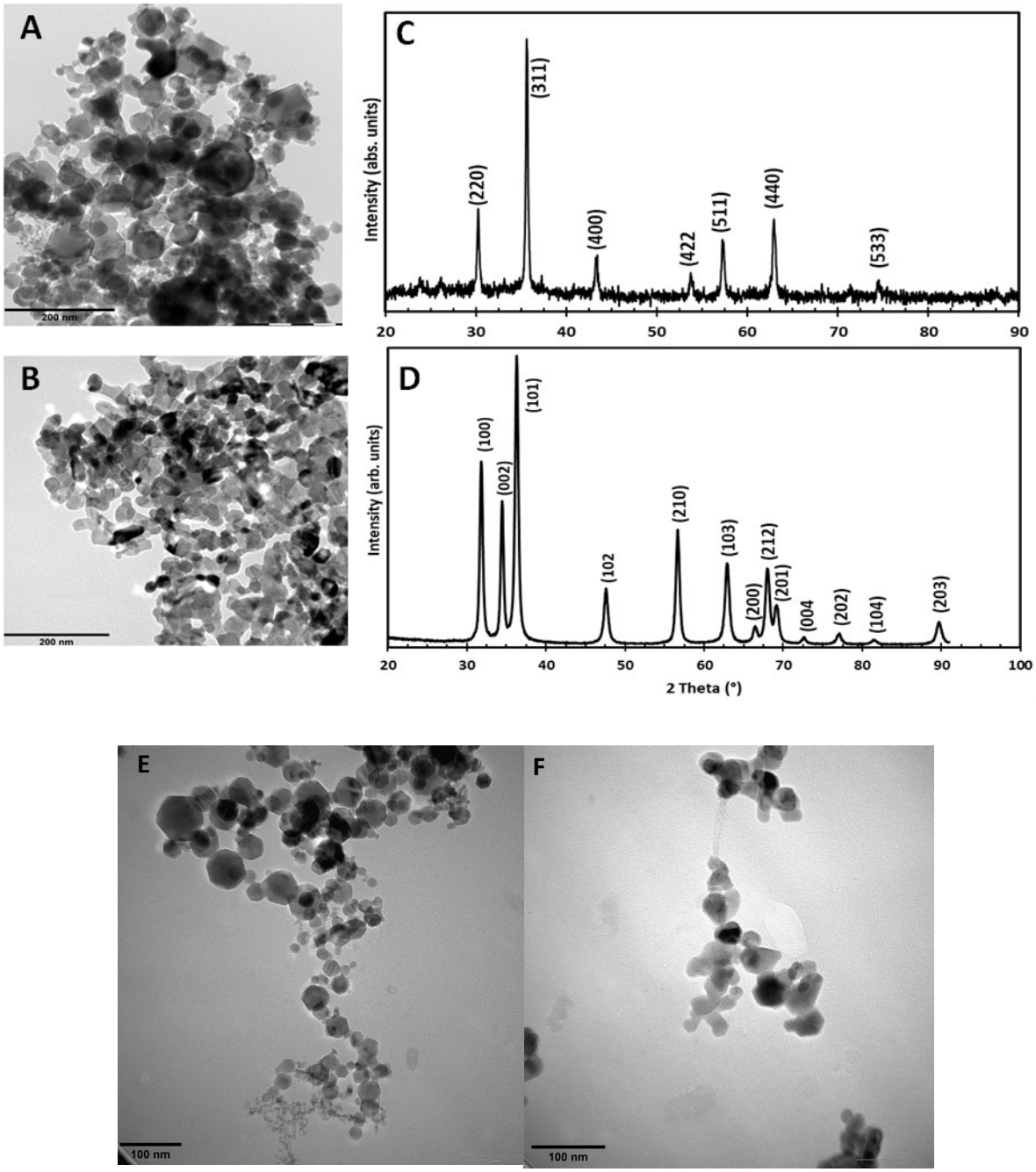

Figure S1 TEM images of (a and e) nFe_2O_3 and (b and f) nZnO. XRD patterns of (c) nFe_2O_3 (d) nZnO.

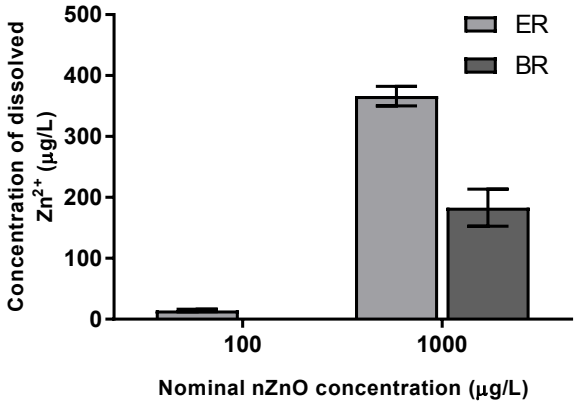

Fig. S2 Dissolved zinc concentrations in the river water samples following 2h incubation under visible light. Errors bars denote standard deviation (n = 3). Concentration of 100 μg L^{-1} ZnO in BR below detection limit (10 μg L^{-1}, not shown). Nominal nZnO exposure concentrations used were 100 and 1000 μg L^{-1}.

Potential interference of ENMs with Live/dead assay kit

In this study, 100% viable cells (standard curve) was used to determine the possible effects the ENPs used in this study could have on the fluorescent probes. We interacted the ENPs and cells at all concentrations, added the SYTO9 (green) and propidium iodide (red) dyes, and incubated for 15 minutes (Tong et al. 2013; Wilke et al., 2016). The fluorescence intensity was then measured using a Flouroskan Ascent FL multimode reader (Thermo Scientific). The level of cell membrane integrity of the ENP interacted cells and non-interacted cells was compared to determine the influence of ENPs on the fluorescence of the Dyes.

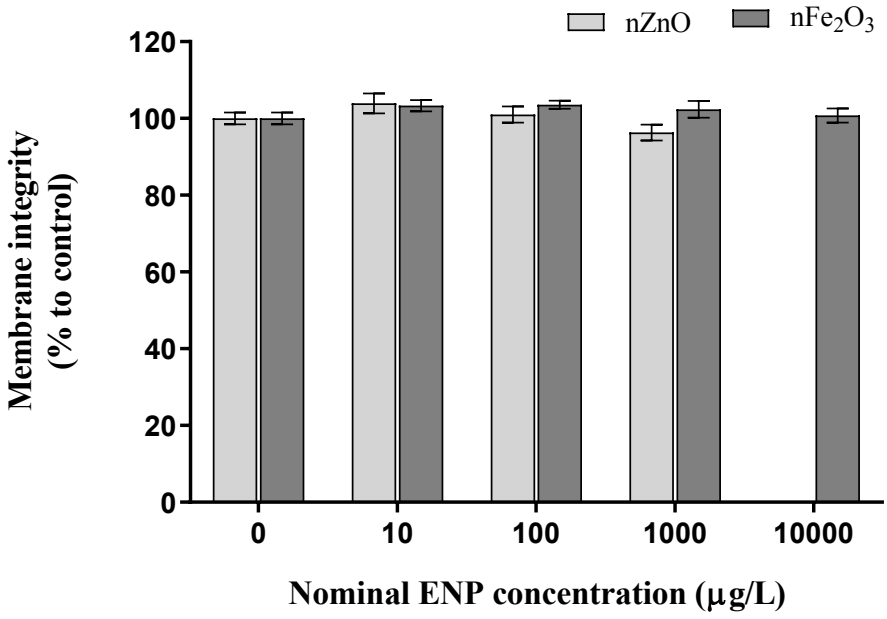

Figure S3: Effects of ENPs on the Live/Dead BacLight assay.

Potential interference of ENPs with ATP assay

To assess the interference of ENPs and ensure the effects observed were due to ENPs and the varying concentrations used in the study, we used a procedure described by Tong et al (2015) and Wilke et al (2016). ENPs were incubated with 100 µl Bactiter-Glo assay reagent for 10 min in the dark. Cell were then added, and the mixture incubated for another 5 min in the dark. Luminescence was recorder on the Flouroskan Ascent FL microplate reader (Thermofisher). Results below show that the assay was not affected by the concentrations of the ENPs used in the study (FigS4).

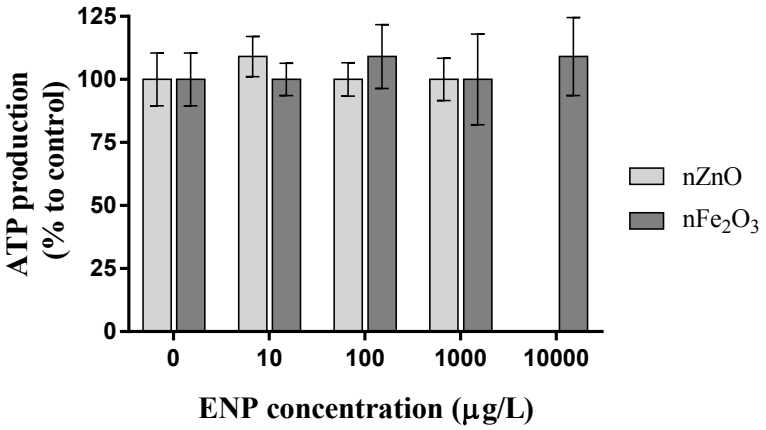

Figure S4 Assessment of ENPs potential interference with the Bactiter Glo assay for ATP production measurement. The luminescence signal produced at all concentrations were not significantly different from the control. The ENPs did not interfere with the assay measurements in this study.

ROS detection assay

A comparison of the intracellular ROS quantification method using DCF-DA as described in Lin et al (2014) was compared to the method used in the study. Both methods did not yield significantly different results.

Herein, the fluorescence intensity of DCF-DA was measured to determine the extent of ROS generation in the water samples alone, or the nanomaterials, in the absence of bacteria. In this study, 150 μL of the tested ENPs concentrations and controls (river water) were transferred to 96-well microplates and incubated with DCF-DA (100 μM final concentration) for 30 min at 37°C under dark conditions (covered with aluminium foil).DCF fluorescence intensity was measured with a Flouroscan Ascent FL microplate reader (ThermoFisher, USA) at an excitation and emission wavelengths of 485 and 538 nm, respectively, to quantify ROS activity both in the water sample and nanomaterial concentrations. ROS production was expressed as percentage fluorescence of the control (minus the ENPS) over the exposed samples. For each test, three replicates of each sample were added per plate, and two plates were used to ensure reproducibility.

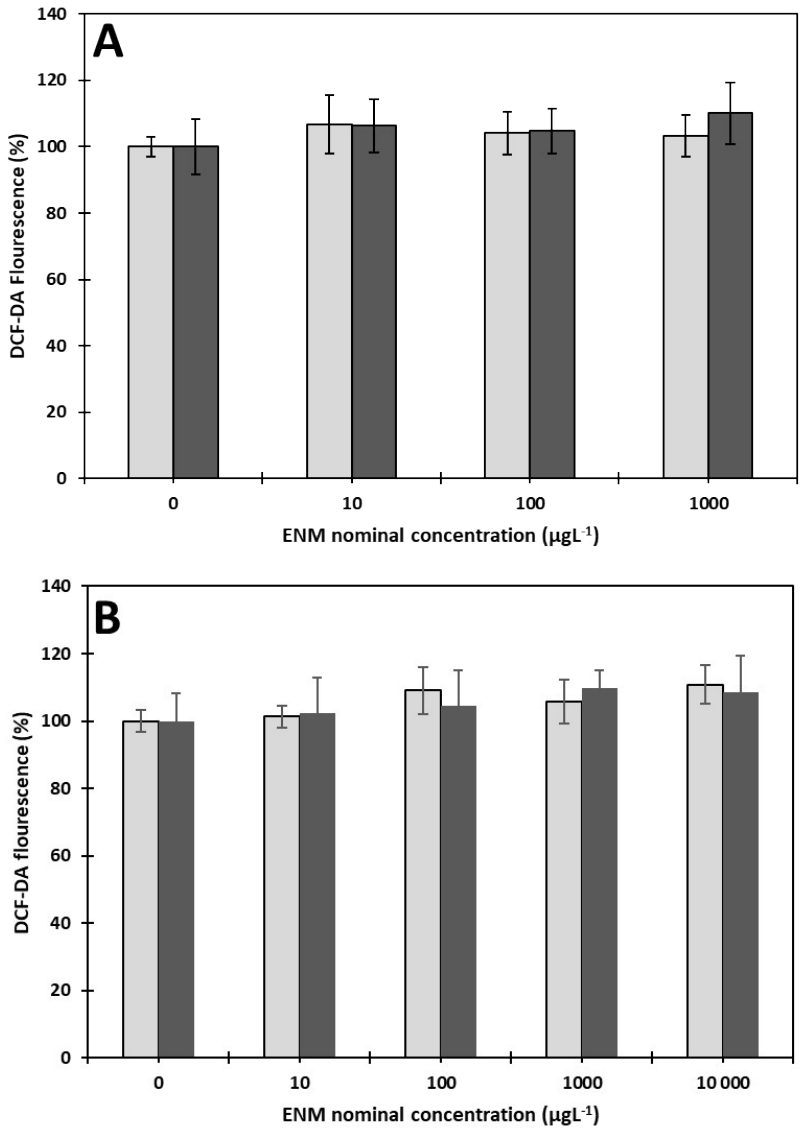

Figure S5: Fluorescence of DCF-DA in water and (a) ZnO nanoparticles and (b) Fe_2O_3 nanoparticles. There was no significant difference in the amount of ROS was produced by the ENMs, showing lack of interference or false positive results.

Microscopic observations of bacterial cells

TEM was used to observe the direct contact between the NPs and the bacterial cells. A drop of the bacteria exposed to the NPs and the NP-free control was air-dried onto a copper grid and was then imaged by the TEM. To observe the internalization and localization of the NPs in the cells and the changes in cellular structure as affected by the NPs, NPs exposed, and non-exposed bacteria were fixed in 2.5% glutaraldehyde, dehydrated in graded

concentrations of ethanol (50%, 70%, 80%, 90%, 95% and 100%) for 15 minutes at each step and transferred to absolute ethanol for 20 minutes. The samples were immersed in 1:1 and subsequent 1:3 mixtures of acetone and epoxy resin for 1 h and 4 h, respectively, and then let to polymerize for 36 h. Ultrathin sections were cut, stained with uranyl acetate and lead citrate and observed with TEM (Huang et al., 2015).

References

Huang, B.Q. and Yeung, E.C., 2015. Chemical and physical fixation of cells and tissues: an overview. In *Plant microtechniques and protocols* (pp. 23-43). Springer, Cham.

Lin, X., Li, J., Ma, S., Liu, G., Yang, K., Tong, M. and Lin, D., 2014. Toxicity of TiO_2 nanoparticles to *Escherichia coli*: effects of particle size, crystal phase and water chemistry. *PloS one*, *9*(10), p.e110247.

Tong, T., Shereef, A., Wu, J., Binh, C.T.T., Kelly, J.J., Gaillard, J.F. and Gray, K.A., 2013. Effects of material morphology on the phototoxicity of nano-TiO2 to bacteria. *Environmental Science & Technology*, *47*(21), pp.12486-12495.

Wilke, C.M., Tong, T., Gaillard, J.F. and Gray, K.A., 2016. Attenuation of Microbial Stress Due to Nano-Ag and Nano-TiO_2 Interactions under Dark Conditions. *Environmetal Science and Technology*, *50*(20), pp.11302-11310.